High order VHS on the surface of a TI using a rotationally symmetric superpotential

Mathew Pareles
Advisor: Jennifer Cano

March 5, 2024

Abstract

The surface states of a 3D topological insulator with a moire superlattice potential have been studied extensively. A moire pattern with 3 or 4-fold rotational symmetry folds the Brillouin zone, creating a divergent density of states and high-order Van Hove singularities, where multiple single VHS overlap. We extend previous analysis to the quasicrystalline case of 5,7,8,...-fold rotationally symmetric superpotentials, which show promise in creating even higher order VHS with $\nu = 4$ instead of $\nu = 3$. We first find the dispersion relation by diagonalizing an approximate matrix representation of the Hamiltonian. We then find the superpotential strength that creates a HOVHS with degenerate perturbation theory analysis.

1 Introduction

Topological insulators are widely studied, and offer insights into superconductivity and topological quantum computing [1] [2] [3]. However, there are gaps in our understanding of the surface states of 3D TIs. With strong interactions, spontaneous symmetry breaking theoretically allows for a gap to open at the surface. For instance, by application of a thin magnetic film [4]. However, there is currently no known TI with a gapped surface. The search for Majorana fermions and gapped topological superconductors for quantum computing is ongoing [3] [4]. We will not focus on this aspect.

Recent progress has been made on understanding TIs in the presence of applied electric potentials, particularly moire superlattices. Twisted layered graphene has been widely studied [5] [6] [7].

Namely, a rotationally or translationally symmetric superpotential folds the Dirac cone in on itself, creating satellite Dirac cones, and allows for divergence in the DOS and Van Hove singularities (VHS) [1] [2]. High order divergences in the DOS lead to high order VHS (HOVHS). Alternately, when many VHS are "folded" together, there is a corresponding HOVHS. By tuning the strength of the potential, we can realize HOVHS. Chandrasekaran et al. considers up to 7 parameters [8]. Using symmetry, all possible VHS points have been classified [9] [8].

HOVHS are highly desired as they show promise towards high temperature superconductivity. For instance, it was shown that the critical temperature diverges polynomially instead of exponentially with the electron-phonon coupling strength [2].

Our goal is to use a rotationally symmetric potential to realize a HOVHS. Other works have used $N = 3, 4, 6$-rotationally symmetric superpotential [2]. However, superpotentials are continuous in space, and there is no reason they must be crystalline. We generalize results to the "quasi-crystalline" case of $N \neq 3, 4, 6$, which can be realized with a gated pattern (but not by a crystal!). Such a pattern has been experimentally achieved for $N = 4, 6$ [10].

We give intuitions on relating HOVHS to the dispersion, and use symmetry to constrain the dispersion. We then search for HOVHS computationally and with perturbation theory.

1.1 Mathematical definitions of our system and VHS

1.1.1 System

Our system is a Dirac cone on the surface of the TI,

$$H_0(\vec{k}) = v\vec{k} \cdot \vec{\sigma} \tag{1}$$

where $\vec{\sigma} = (\sigma_x, \sigma_y)$ is the fermion spin-basis. The eigenvalues are $E(\vec{k}) = \pm v|\vec{k}|$. We arbitrarily choose a dot product instead of e.g. a cross product. Thus, spins align with momentum.

We also have an N-fold rotationally symmetric potential. To be concrete, we choose it to have the form,

$$U(\vec{r}) \equiv 2W \sum_{n=0}^{N-1} \cos(\vec{Q}_n \cdot \vec{r}) \tag{2}$$

$$\vec{Q}_n \equiv Q(\cos(2\pi n/N), \sin(2\pi n/N)) \tag{3}$$

We identify $\vec{Q}_n$ as the fundamental reciprocal lattice vectors. Note the potential is always even-fold symmetric, as the cosine treats Q_n and $-Q_n$ the same. There is no loss of generality, as $2n$-fold symmetric potentials have the same low energy dispersion as n-fold symmetric potentials, as is seen using perturbation theory. As expected, the potential will be periodic for $N = 1, 2, 3, 4, 6$, and will be quasicrystal-like for all other values of N.

There are two relevant physical quantities, v and W. By writing the W in terms of v, we fully determine the system.

1.1.2 Intuition on DOS and VHS

Our goal is to to find neighborhoods of k-points where the DOS is discontinuous or diverges, known as a Van Hove Singularity (VHS). We see that this happens when the dispersion has high-order k dependence.

The density of states (DOS) are defined as,

$$g(E) \equiv \int_{R^d} \frac{d^d k}{(2\pi)^d} \delta(E - E(\vec{k})) \tag{4}$$

For intuition, let us find VHS for the simple dispersion $E \sim k^\nu$ where $d = 2$ dimensions.

We see that $d^2\vec{k} \sim kdk$, and $k \sim E^{(1/\nu)}$. After integrating, we have

$$g(E)_{(2D)} \sim E^{(2/\nu)-1} \tag{5}$$

If $\nu > 2$, the DOS $g(E)$ diverges for certain E and corresponding k (namely $k = 0$, where the dispersion is flattest). This divergence is known as high-order Van Hove Singularity (HOVHS). We see that in general, the greater the leading order power, the greater the divergence. The lowest order that has interesting behavior is $\nu = 2$. This is a "regular" VHS (a discontinuity in $g(E)_{(2D)}$, but no divergence).

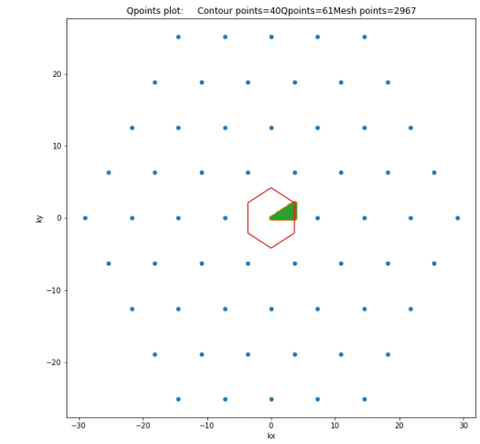

(a)

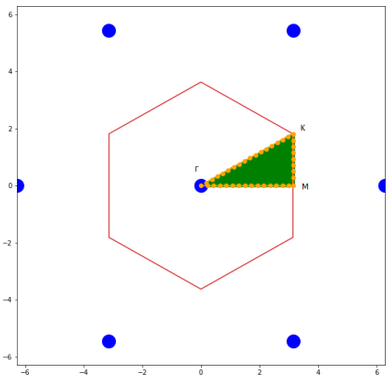

(b)

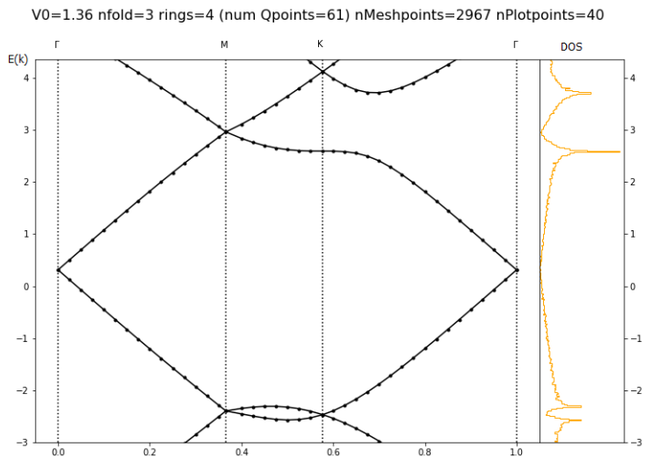

(c)

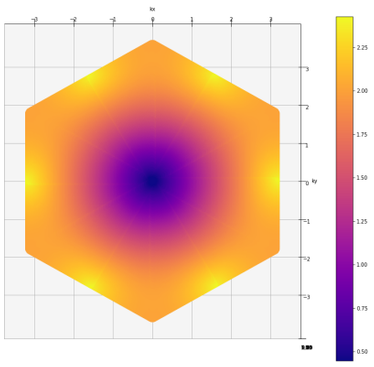

(d)

Figure 1: Here we find a HOVHS with $N = 3$ and $W = 1.36$. a) Setup of $N = 3$, $R = 4$ calculation b) Close-up of (a). HOVHS should be on lines of high symmetry (ΓM or $K\Gamma$), so we look for flat bands on these contours. c) Band calculation for the setup shown in (a), (b). At $W = 1.36$, the band is flat at K, and high-order divergence of the DOS at $E(K)$. Compare to [2] Figure 1b. d) Fermi surface calculated at $W = 1.36$. Note with units $W = 1.36\hbar v/L$, and $Q \equiv 2\pi/\tilde{L}$, where $\tilde{L}$ is some multiple of the real lattice spacing L. In the $N = 3$ case, $\tilde{L} = \frac{\sqrt{3}}{2}L$.

Let us now consider an arbitrary dispersion about the point $\vec{K}$,

$$E(\vec{k}) = E_{\vec{K}+\vec{k}} - E_{\vec{K}} \tag{6}$$

$$= \Omega_x k_x + \Omega_y k_y + \alpha_{xx} k_x^2 + \alpha_{yy} k_y^2 + \alpha_{xy} k_x k_y + ... \tag{7}$$

We expect the condition for divergent DOS (and HOVHS) at $\vec{K}$ to be that first and second order terms vanish,

$$\Omega = 0 \tag{8}$$

$$\alpha = 0 \tag{9}$$

Each coefficient necessarily depends on the physical parameters of the system, like superpotential strength W, Dirac cone strength v, and location of fundamental reciprocal lattice points Q.

HOVHS are realized experimentally by tuning W, v, Q. For instance, can try for $\alpha(W, v, Q) \to 0$, though zeros are not guaranteed.

1.1.3 HOVHS formal definition

Let us define HOVHS more formally. We see that it is compatible with our intuitions.

A HOVHS is present at $\vec{K}$ if $\vec{\nabla}E|_{\vec{K}} = \vec{0}$ (it is a regular VHS) and also if $det(D = 0)$, where $D_{ij} = \partial_i \partial_j E|_{\vec{K}}$.

$$\vec{\nabla}E|_{\vec{K}} = \vec{0} \tag{10}$$
$$det(D = 0) \tag{11}$$

1.2 Finding HOVHS with symmetry

We constrain our system to have N-fold rotational symmetry. This limits the dependencies of the coefficients in (7), and thus satisfies (10) and (11) more easily, allowing for HOVHS.

Note that this result is quite exhaustive, as it is difficult to think of other symmetries besides rotational (translational symmetry is just a lattice). One could consider other constraints that are not symmetries, but that is very open-ended.

Our constraint is now,

$$E_N(\vec{k}) = E_N(\hat{R}_{(2\pi n/N)} \cdot \vec{k}) \tag{12}$$
$$R_\phi : \begin{cases} k_x \to k_x \cos(\phi) + k_y \sin(\phi) \\ k_y \to k_y \cos(\phi) - k_x \sin(\phi) \end{cases} \tag{13}$$

When rotational symmetry is present, often mirror symmetry is also present, and we choose reflections about the x-axis to be invariant. This gives an additional constraint,

$$E(k_x, k_y) = E(k_x, -k_y) \tag{14}$$

Let's determine how (12-14) constrain the arbitrary dispersion (7). See Appendix A.I for details.

Mirror symmetry (14) constrains the dispersion be even in k_y,

$$E(\vec{k}) = \Omega_x k_x + \alpha_x k_x^2 + \alpha_y k_y^2 + ... \tag{15}$$

Rotational symmetry (12) is more complicated. The trick it to enforce symmetry with a sum,

$$E_N(\vec{k}) \sim \sum_{n=0}^{N-1} E_N(R_{\frac{2\pi n}{N}} \vec{k}) \tag{16}$$

We can see that all rotationally-symmetric dispersions have a 2nd order, isotropic leading term (Appendix A.I),

$$E_N(\vec{k}) = \alpha k^2 + ... \tag{17}$$

More generally, for a given N, dispersions are even and isotropic only up to order N,

$$E_N(\vec{k}) = \alpha k^2 + \beta k^4 + \gamma k^6 + ... + \kappa k_x^N + \lambda k_x^{N-1} k_y + ... \tag{18}$$

We have confirmed this computationally for $N, x < 10$, where x is the power of k^x. A general proof remains to be done.

This gives two important results,

1) At rotationally symmetric points, we expect to create a HOVHS by tuning only a single parameter W, so that $\alpha(W) \to 0$. Compare this to the arbitrary dispersion (7), where we expect to tune around 5 parameters to make all 5 coefficients vanish.

2) We do not expect extremely high-order VHS to come from high N-fold rotationally symmetric potentials, as we always have a leading second order term in the dispersion. We can still expect lower order HOVHS (a step up from VHS).

We are now convinced that rotational and mirror symmetries create HOVHS more easily. Assuming such symmetry, we will search for the values of superpotential strength W that create HOVHS.

Note: One limitation of this approach is assuming HOVHS are near high-symmetry points. There might be some 'magic' point far away where divergences occur. We have also been using the intuition that the presence of fewer coefficients means HOVHS are more easily tuned, but must prove this. See Appendix A.II.

2 Analytical result

Let us derive the Hamiltonian in the k-basis.

We find the superlattice potential contribution from (2). $U(\vec{r})$ contributes symmetrically to both spin-up and spin-down particles, and thus in spin-basis is $H \sim U(\vec{r})\sigma_0$. Thus,

$$\hat{H}^W = \int_{allspace} d^2\vec{r}\, U(\vec{r})(\sigma_0)_{\sigma,\sigma'}\ |\vec{r},\sigma\rangle\langle\vec{r},\sigma'| = \int_{allspace} d^2\vec{r}\, U(\vec{r})\,|\vec{r},\sigma\rangle\langle\vec{r},\sigma| \tag{19}$$

$$= \int_{allspace} \frac{d^2\vec{k}}{(2\pi)^2}\frac{d^2\vec{k}'}{(2\pi)^2}\,|\vec{k}',\sigma\rangle\langle\vec{k},\sigma| \sum_{\vec{Q}=\vec{Q}_0}^{\vec{Q}_N} W\left[\frac{1}{V}\int_{allspace} d^2\vec{r}\, e^{-i\vec{Q}\cdot\vec{r}}e^{i(\vec{k}'-\vec{k})\cdot\vec{r}}\right] + \quad H.c. \tag{20}$$

$$= \int_{allspace} \frac{d^2\vec{k}}{(2\pi)^2}\left[W\sum_{\vec{Q}}|\vec{k}+\vec{Q},\sigma\rangle\langle\vec{k},\sigma|\right] \quad + H.c. \tag{21}$$

$$= \int_{(pseudo)unitcell} \frac{d^2\vec{k}}{(2\pi)^2}\left[W\sum_{\vec{Q},\,\vec{G}}|\vec{k}+\vec{Q}+\vec{G},\sigma\rangle\langle\vec{k}+\vec{G},\sigma|\right] + \quad H.c. \tag{22}$$

Where $\vec{G}$ is the reciprocal lattice $\sum_i n_i\vec{Q}_i$ and n_i are all integers, and a sum over repeated σ implied. We identify the integrand in the final line to be the Hamiltonian density in k-space, $H^W(\vec{k})$.

Similarly, the term from the massless Dirac fermion (1) is

$$\hat{H}^v = \int_{allspace} \frac{d^2\vec{k}}{(2\pi)^2}(H_0(\vec{k}))_{\sigma,\sigma'}\,|\vec{k}\ \sigma\rangle\langle\vec{k}\ \sigma'| \tag{23}$$

$$= \int_{(pseudo)unitcell} \frac{d^2\vec{k}}{(2\pi)^2}\left[\sum_{\vec{G}}(H_0(\vec{k}+\vec{G}))_{\sigma,\sigma'}\,|\vec{k}+\vec{G},\sigma\rangle\langle\vec{k}+\vec{G},\sigma'|\right] \tag{24}$$

We then have

$$H^v(\vec{k}) = \sum_{\vec{G}}(H_0(\vec{k}+\vec{G}))_{\sigma,\sigma'}\,|\vec{k}+\vec{G},\sigma\rangle\langle\vec{k}+\vec{G},\sigma'| \tag{25}$$

$$H^W(\vec{k}) = W\sum_{\vec{Q},\,\vec{G}}|\vec{k}+\vec{Q}+\vec{G},\sigma\rangle\langle\vec{k}+\vec{G},\sigma| \ + \ H.c. \tag{26}$$

$$H(\vec{k}) = H^v(\vec{k}) + H^W(\vec{k}) \tag{27}$$

The eigenenergies of $H(\vec{k})$ are the dispersion $\{E_{\vec{k}}\}$ at a particular $\vec{k}$.

This Hamiltonian holds exactly for quasicrystals at low energies, when the Brillouin zone never folds back on itself. Thus in the low energy domain, we expect this Hamiltonian holds for all N, where the (pseudo)Brillouin zone is constructed from Voronoi cells as in the crystalline case.

3 Computational result: approximation

In this section we replicate results in [2]. We calculate the dispersion and DOS for a given N-fold symmetric potential with potential strength W.

For lattice-generating N, one can construct the Brillouin zone (BZ) naturally, which is just a Wigner–Seitz cell (indicated by red lines). We extend this construction to systems with quasilattice-generating values of N. This BZ helps us define relevant contours and meshes to compute over.

Our process is 1) choose an N and W 2) choose appropriate details relevant to the computation, which are the number of rings R (indicated by blue points), the mesh of k points for computing the DOS (indicated by green points), and the contour for computing the band structure (indicated by orange points).

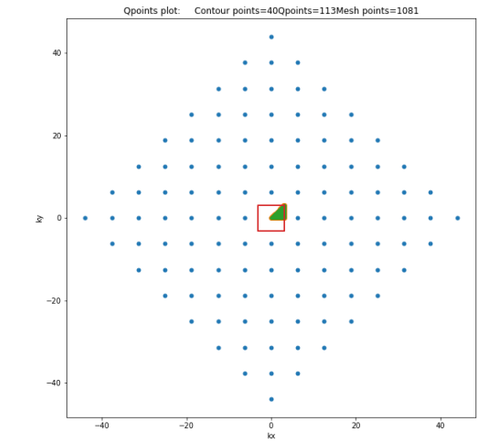

(a)

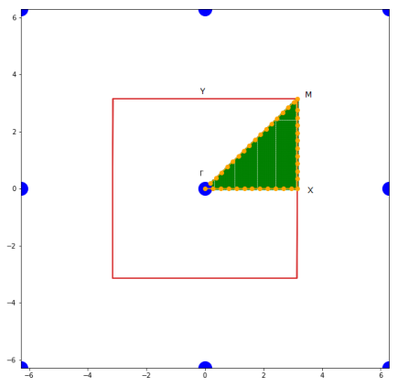

(b)

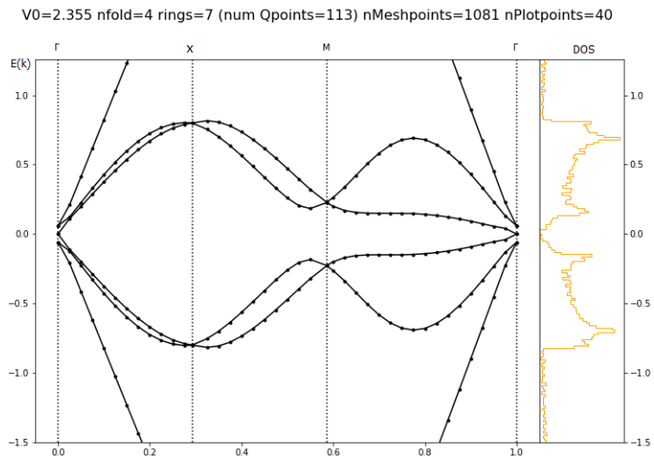

(c)

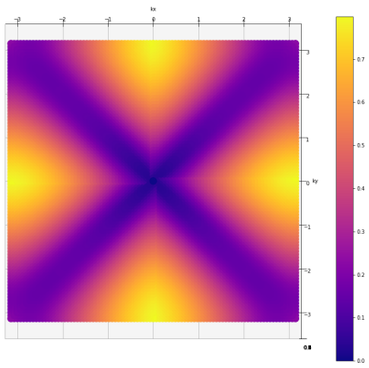

(d)

Figure 2: Here we find a HOVHS with $N = 4$, $W = 4.71/2 = 2.355$ (half the potential found by [2]), since we twice the amount of Q's. This is just a detail). a) Setup of $N = 4$, $R = 7$. I needed at least 6 rings for the calculation to stabilize. b) Close-up of (a). c) Band calculation for $W = 2.355$. There are 4 divergences of the DOS, and on the $M\Gamma$ line is a HOVHS. Compare to [2] Figure 7b. d) Fermi surface.

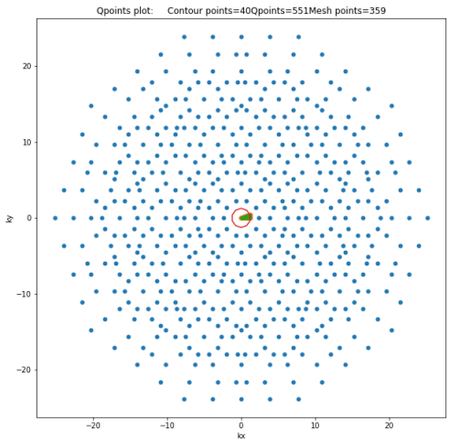

(a)

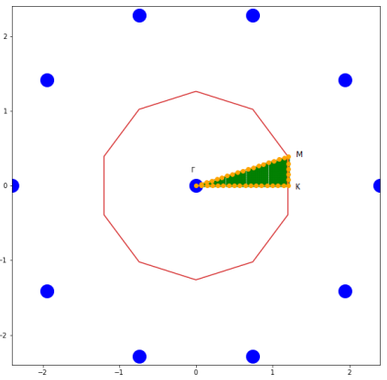

(b)

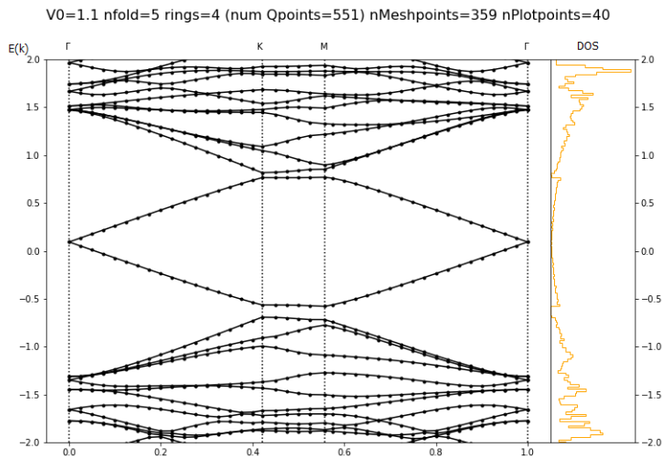

(c)

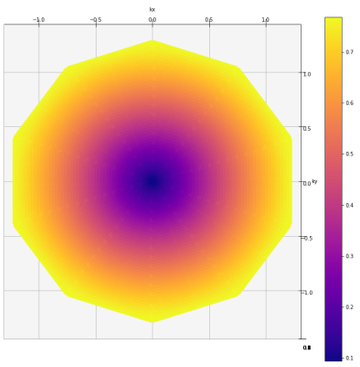

(d)

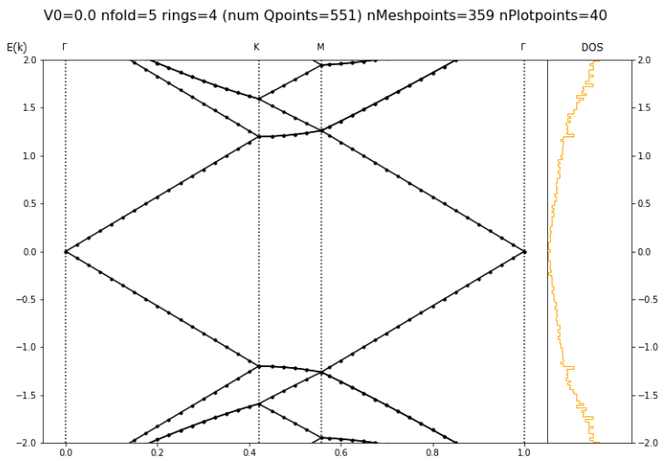

(e)

Figure 3: Here we unsuccessfully look for HOVHS with $N = 5$, $R = 4$. This is our first quasicrystal-like example. a) Setup of $N = 5$, $R = 4$. There are many more unique $\vec{G}$ points than before, since $\vec{Q}_i + \vec{Q}_j \neq \vec{Q}_k$ where $i \neq j \neq k$. b) Close-up of (a). As a result of two Q's not adding to some third Q, the innermost ring is not of distance Q to the origin, but instead of some smaller distance $\min |\sum_i n_i \vec{Q}_i|$. We base our BZ on this innermost ring (dependent on the computational parameter R which has no physical relevance!). In (c-d) I consider $W = 1.1$ c) I slowly increased the potential W to see if the DOS would contain divergences as before. Note that the band structure of a quasilattice is not well-defined, but can be used to gain intuition. The first significant change from Dirac-cone occured at $W = 1.1$. However, we see that there is no flattening of bands. Instead, a gap opens up, which violates TR symmetry and indicates that our perturbation is no longer valid. d) Fermi surface, with fairly trivial behavior. e) Band structure and DOS with zero potential strength ($N = 5$, $W = 0$).

From Figure 3, our perturbation starts to break down before a HOVHS forms. However, there are many possible issues including:

1) Building in rings is too inefficient. For instance, $N = 4$ requires a high number of cutoff $\vec{G}$ points (6 rings), but there are other definitions of the cutoff that require fewer points. The number of points grows exponentially with the number of rings for $N = 5$ and it is not viable to use more than a few rings.

2) It is possible our architecture of building 'rings' poorly represents quasilattices. The quasilattice set $\vec{G}$ densely fills all space, and we are only tiling some finite subset. Deeper analysis such as [11] may be needed.

3) We may need to sample k-points differently when computing DOS. The Wigner-Seitz construction may not be appropriate.

There are many possible computation issues, and so we move to perturbation theory.

4 Perturbation approach

Let us view our system (27) from the lens of degenerate perturbation theory. We have a Dirac cone which will produce circular rings of degenerate points. At certain distances from the origin, there will be some number of degenerate points (typically N) separated by fundamental reciprocal lattice vectors $\vec{Q}_n$. See Figure 4. We can analyze this using degenerate perturbation theory. We closely follow the approach in [1], and compare our results to [2].

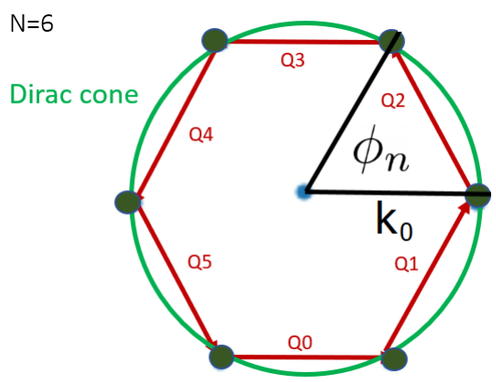

Figure 4: The perturbation in W considers N degenerate states coupled by fundamental reciprocal lattice vectors Q_n.

4.1 Procedure

4.1.1 Perturbing in W

We must first find the degenerate eigenstates. For the spin Hamiltonian, (1), the eigenstates are,

$$|\pm e^{i\phi_{\vec{k}}}\rangle \equiv \frac{1}{\sqrt{2}}(1, \pm e^{i\phi_{\vec{k}}}) \tag{28}$$

The eigenstates of the total Hamiltonian are then

$$|\vec{k}, \pm\rangle = |\vec{k}\rangle \times |\pm e^{i\phi_{\vec{k}}}\rangle \tag{29}$$

$$\phi_{\vec{k}} \equiv \arctan(k_y, k_x) \tag{30}$$

We can now calculate the degenerate states. They are located at $\vec{k}_n = k_0(\cos(2\pi n/N), \sin(2\pi n/N))$, where $k_0 = \frac{Q}{2}\frac{1}{\sin(\pi/N)}$ and $n = 0, 1, ..., N-1$ (obvious from Figure 4) For simplicity, we also only consider positive energy states, which do not interact with negative energy states. Thus, the (positive energy) degenerate states are

$$|n\rangle \equiv |\vec{k}_n, +\rangle = |\vec{k}_n\rangle \times |e^{i\phi_n}\rangle \tag{31}$$

$$\phi_n \equiv \phi_{\vec{k}_n} = 2\pi n/N \tag{32}$$

We can now compute the perturbing Hamiltonian, assuming small potential strength W. There will be a contribution from the Dirac cone and potential, so

$$H_N = H_N^v + H_N^W \tag{33}$$

We start with the Dirac cone term (25). To first order in W,

$$H_N^v = v\sum_{n=0}^{N-1} |\vec{k}_n| \ \langle n|n\rangle \, |n\rangle \langle n| \tag{34}$$

$$= v\sum_{n} |\vec{k}_n| \ |n\rangle \langle n| \tag{35}$$

And the contribution from our potential (26) is (again to first order in W),

$$H_N^W = \sum_{n=0}^{N-1} V_{(\vec{k}_{n+1}-\vec{k}_n)} \ \langle n+1|n\rangle \, |n+1\rangle \langle n| + H.c. \tag{36}$$

$$= W \sum_{n=0}^{N-1} \langle n+1|n\rangle \, |n+1\rangle \langle n| + H.c. \tag{37}$$

$$= W \sum_{n=0}^{N-1} \frac{1}{2}(1 + e^{-i(\phi_{n+1}-\phi_n)}) \, |n+1\rangle \langle n| + H.c. \tag{38}$$

$$= W \sum_{n} \ e^{-i\frac{(\phi_{n+1}-\phi_n)}{2}} \cos\frac{(\phi_{n+1}-\phi_n)}{2} \, |n+1\rangle \langle n| + H.c. \tag{39}$$

One can simplify using $|\vec{k}_n| = k_0$ and $\phi_a - \phi_b = \phi_{a-b}$, but it will be useful shortly to leave everything unsimplified.

4.1.2 H_N dispersion

From H_N, one can calculate the energy spectrum $\{E_j\}_{j=0,\ldots,N-1}$ at these N degenerate points. H_N is diagonalized in the Fourier or "j-basis",

$$|n\rangle = \frac{1}{\sqrt{N}} \sum_{j=0}^{N-1} e^{-\frac{2\pi i n}{N} j} \, |j\rangle \tag{40}$$

The energy of the jth state can be easily confirmed,

$$E_j = vk_0 + 2W \cos(\pi/N) \cos(2\pi(j + \frac{1}{2})/N) \tag{41}$$

We see that the states $|j\rangle$ and $|-1-j\rangle$ are degenerate. Note the states $|n\rangle$ and $|j\rangle$ are defined modulo N. Both the potential and Dirac cone are TR symmetric, so degeneracies are protected by TR symmetry.

4.1.3 H_N analysis

We have solved and analyzed the energy spectrum at specific points $\vec{k}_n$. We more generally want the dispersion $\{E_n(\vec{k})\}$ when moving some small vector $\vec{k}$ away from these points.

Thus, we need another perturbation in k-space to find $H_{N,\vec{k}}$.

Still, we can find intuition from H_N alone. If $W \gg k_0$, equation (41) implies the bands will have large spacing, so the only relevant coupling is between degenerate states. Then the dispersion $E_{N,\vec{k}}$ can be equated with the coupling of degenerate states $\langle -j-1| \, H_{N,\vec{k}} \, |j\rangle$. We will find that the leading order of this coupling k^ν increases with N. Thus, we expected to find arbitrarily large HOVHS.

There are two subtle flaws in this argument. We will see second order perturbation theory requires coupling outside (not inside) degenerate blocks. Also, our perturbation assumed $W \ll k_0$, and it is unclear if the extension to $W \gg k_0$ will hold.

4.1.4 Perturbing in k

We must consider moving some small distance $\vec{k} \equiv k(\cos(\phi_{\vec{k}}), \sin(\phi_{\vec{k}}))$ from our degenerate $\vec{k}_n$ points, where we define small k to mean $k \ll |\vec{k}_n|$. Degenerate PT strongly constrains this process, as all states must remain separated by some fundamental reciprocal lattice vector $\vec{Q}$. See Figure 5.

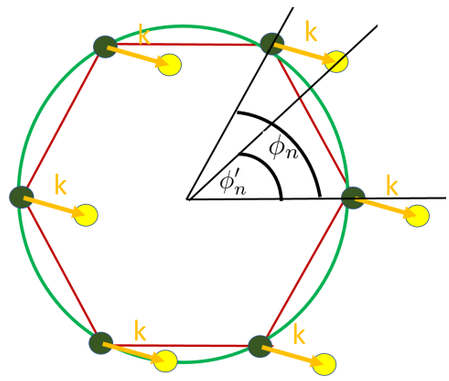

Figure 5: The perturbation in k-space takes the states $\vec{k}_n \to \vec{k}' = \vec{k}_n + \vec{k}$, with new angle ϕ'_n

This transformation requires for all $n = 0, ..., N-1$,

$$\vec{k}_n \to k'_n = \vec{k}_n + \vec{k} \tag{42}$$

Thus we must make the substitutions,

$$\phi_n \to \phi'_n = \arctan\left(\frac{k_0 \sin(\phi_n) + k \sin(\phi_{\vec{k}})}{k_0 \cos(\phi_n) + k \cos(\phi_{\vec{k}})}\right) \tag{43}$$

$$|\vec{k}_n| \to |\vec{k}'_n| = \sqrt{(k_0 \cos(\phi_n) + k \cos(\phi_{\vec{k}}))^2 + (k_0 \sin(\phi_n) + k \sin(\phi_{\vec{k}}))^2} \tag{44}$$

$$\begin{aligned} |n\rangle \to |n'\rangle &= |\vec{k}'_n, +\rangle = |\vec{k}_n + \vec{k}, +\rangle \\ &\equiv \frac{1}{\sqrt{N}} \sum_{j=0}^{N-1} e^{-\frac{2\pi i n}{N} j} \, |j'\rangle \end{aligned} \tag{45}$$

To find the perturbing Hamiltonian, one substitutes (43-45) into H_N^v (35) to find $H_{N,\vec{k}}^v$, and into H_N^W (39) to find $H_{N,\vec{k}}^W$. Again, summing the two terms gives the total Hamiltonian.

4.2 Result

We apply the above substitutions, and expand a power series in $K = \frac{k}{k_0} \ll 1$. The result in the j-basis is (see Appendix B for thorough derivation),

$$H_{N,\vec{k}}^v = v k_0 \sum_{m=0}^{\infty} \sum_{x=m}^{2m} K^x \sum_{\substack{z=2m-x, \\ 2m-x-2, \\ 2m-x-4, \\ \dots}}^{z \geq 0} [const.] e^{-1\phi_{\vec{k}} z} \sum_{j=0}^{N-1} |j+z\rangle \langle j| + H.c. \tag{46}$$

$$H_{N,\vec{k}}^{W\,(x\geq 1)} = W \frac{e^{-\frac{2\pi i}{N}}}{2} \sum_{x=1}^{\infty} K^x \sum_{j,j'=0}^{N-1} e^{-\frac{2\pi i}{N} j'} \, |j'\rangle \langle j| \left[\frac{1}{N} \sum_{n=0}^{N-1} e^{-\frac{2\pi i n}{N}(j'-j)} \chi_{n,\vec{k}}(x)\right] + H.c. \tag{47}$$

Where we have defined (Appendix B, "H^W term")

$$\chi_{n,\vec{k}}(x) \equiv \sum_{\substack{\text{all } p_x = \{(i,d_i)\}_i \\ \text{s.t. } i,d_i > 0 \\ \sum_i i \cdot d_i = x}} \prod_{(i,d_i) \in p_x} [const.] (c_{n,\vec{k}}(i))^{d_i} \tag{48}$$

$$c_{n,\vec{k}}(j) \equiv \cos[j(\phi_{\vec{k}} - \phi_n - \frac{\pi}{N})] \tag{49}$$

And there is a useful orthogonality relation (Appendix B, "orthogonality")

$$\left[\frac{1}{N} \sum_{n=0}^{N-1} e^{-\frac{2\pi i n}{N}(j'-j)} \left[c_{n,\vec{k}}(M)\right]^L\right] = \sum_{\substack{z=L, \\ L-2, \\ L-4, \\ \dots}}^{z \geq 0} [const.] \cdot e^{-i(\phi_{\vec{k}} - \frac{\pi}{N}) M z} \cdot \delta_{(Mz = j'-j)} + [''z \to -z] \tag{50}$$

Here [*const.*] denotes variables that are unimportant and can be treated as constant.

We equated the coupling between degenerate states with the dispersion, $\langle -j-1|\, H_{N,\vec{k}}\, |j\rangle \sim E_{N,\vec{k}}$. We hoped that with large N, this dispersion would be high order in K. This naively appears to be true - the leading order term for the coupling between states $|j\rangle$ and $|j+z\rangle$ goes as their difference K^z.

This is true for (46), as $x \leq m$, $z \leq 2m - x$, so $z \leq x$.

This is also true for (47), but requires more work: We want to show for a given coupling x, the minimal order present is K^x. We can prove this the other way around - for a given K^x we want to show the maximal coupling is x. Proof requires use of $\chi_n(x)$, which fully determine couplings. We notice two points,

1) The decomposition of $\chi(x)$ has terms of the form $c(m)^l$, where $ml \leq x$. Proof: the coefficients of K^x are $\chi(x) \sim c(a)^{x_1}c(b)^{x_2}c(c)^{x_3}...$ s.t. $x = ax_1 + bx_2 + cx_3 + ...$ Using $c(a)c(b) \sim c(a+b) + c(a-b)$, we can easily confirm this.

2) The term $c(m)^l$ contributes a maximal coupling of ml. Proof: from (119), $j' - j \leq ml$.

Clearly the maximal coupling for a term of order K^x is x.

Thus, we have that large N gives large couplings, and thus (incorrectly) conclude that there are arbitrarily high order dispersions and HOVHS.

4.3 Confirming TR invariance

Time reversal symmetry holds for both the Dirac cone and the superpotential. It should hold for the total Hamiltonian.

We do a sanity check for the simple case of $N = 2$ to prove our result is TR invariant. We have two fundamental reciprocal lattice vectors $\vec{k}_0 = -\vec{k}_1$, and a Hamiltonian $H_{2,\vec{k}}$ written as $H_{\vec{k}}$. The TR operator, T, should satisfy,

$$TH_{\vec{k}}T^{-1} = H_{-\vec{k}} \tag{51}$$

Let us confirm this. By definition, the TR operator satisfies,

$$T\,|\vec{k},+\rangle = e^{-i\phi_{\vec{k}}}\,|-\vec{k},+\rangle \tag{52}$$

$$TcT^{-1} = c^* \tag{53}$$

It is easy to show

$$\langle e^{\phi_{k_0+k}}|e^{\phi_{k_1+k}}\rangle \sim \sum_{m=1}^{\infty}(i)^m \sin^m(\phi_{\vec{k}})K^m \tag{54}$$

$$H_{\vec{k}} = \sum_{m=1}^{\infty} |k_0+k\rangle\, i^m \sin^m(\phi_{\vec{k}})K^m\, \langle k_1+k| + H.c. \tag{55}$$

We confirm for our Hamiltonian,

$$TH_{\vec{k}}T^{-1} = \sum_m |k_1-k\rangle\, (-i)^m \sin^m(\phi_{-\vec{k}})K^m\, \langle k_0-k| + H.c. \tag{56}$$

$$\sum_m |k_0-k\rangle\, (i)^m \sin^m(\phi_{-\vec{k}})K^m\, \langle k_1-k| + H.c. \tag{57}$$

$$= H_{-\vec{k}} \tag{58}$$

4.4 Explicit calculation

To proceed with this analysis, we must consider the form of the Hamiltonian.

We can find the matrix form of $H_{N,\vec{k}}$ using mathematica. $H^v_{N,\vec{k}}$ is found using (46). $H^W_{N,\vec{k}}$ requires more work from (47), see Appendix B "decomposition", Equation 125).

When computing a particular matrix, we choose:
1) The symmetry $N = N_0$
2) The order $O(K)$ beyond which terms in $H_{N,\vec{k}}$ are truncated (a computational detail)

We also assume the j-basis is ordered in degenerate pairs $\{|0\rangle, |N-1\rangle, |1\rangle, |N-2\rangle, ...\}$.

For instance, $N = 3$, $O(K) = 1$ and j-basis $\{|0\rangle, |2\rangle, |1\rangle\}$ yields

$$H_{N,\vec{k}} = \begin{pmatrix} k_0 v + \frac{W}{2} & \frac{1}{4} e^{-i\phi_{\vec{k}}} (2k_0 v + 3W) K & \frac{1}{2} e^{i\phi_{\vec{k}}} k_0 v K \\ \frac{1}{4} e^{i\phi_{\vec{k}}} (2k_0 v + 3W) K & k_0 v + \frac{W}{2} & \frac{1}{4} e^{-i\phi_{\vec{k}}} (2k_0 v - 3W) K \\ \frac{1}{2} e^{-i\phi_{\vec{k}}} k_0 v K & \frac{1}{4} e^{i\phi_{\vec{k}}} (2k_0 v - 3W) K & k_0 v - W \end{pmatrix} \tag{59}$$

It is more useful to consider the non-zero entries at each order of K (shown in black),

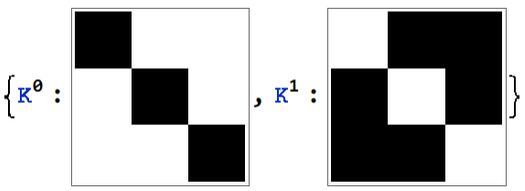

See Figure 6 for the general case ($O(K) = 6$).

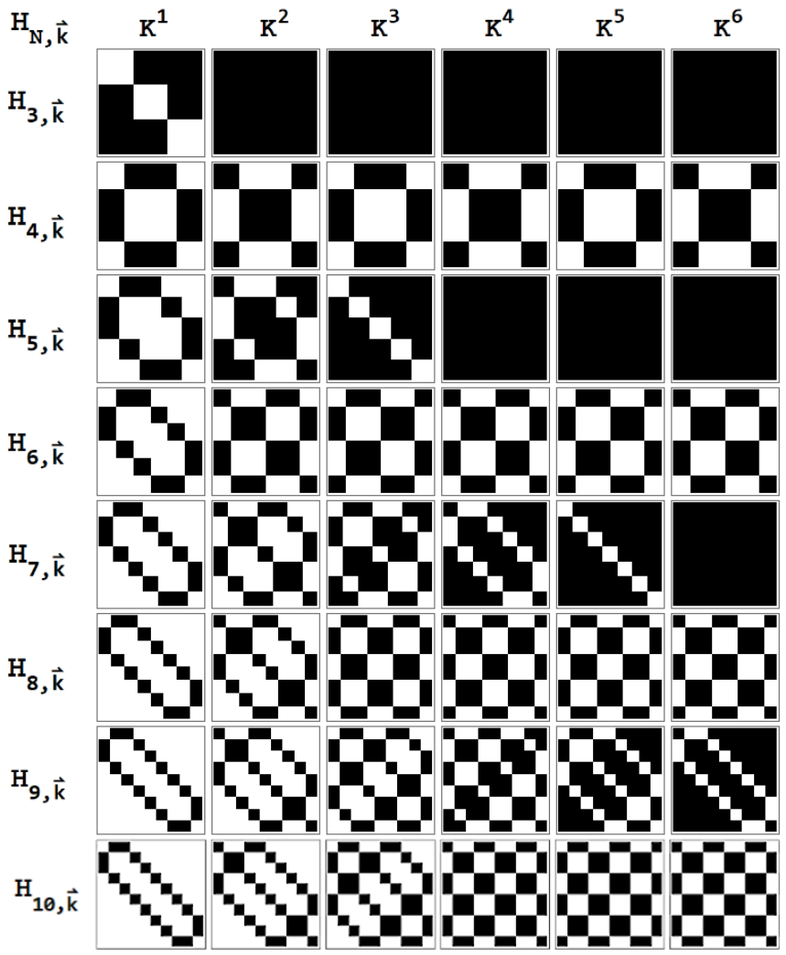

Figure 6: The perturbation Hamiltonian of various N-fold rotational symmetries, up to order $O(K) = 6$. Each row i in this diagram ($H_{i,\vec{k}}$) is a different Hamiltonian. Each column j is a the matrix contribution of a given order of $K = (\frac{k}{k_0})^j$ (white elements are zero, black elements involve $k_0 v$, W, and $\phi_{\vec{k}}$). The Hamiltonian of a given row is found by summing over all the columns.

4.5 Dispersion from PT

We find that the dispersion always has a leading second order term K^2, using degenerate PT on the blocks. All first order terms take a similar form. See Figure 7.

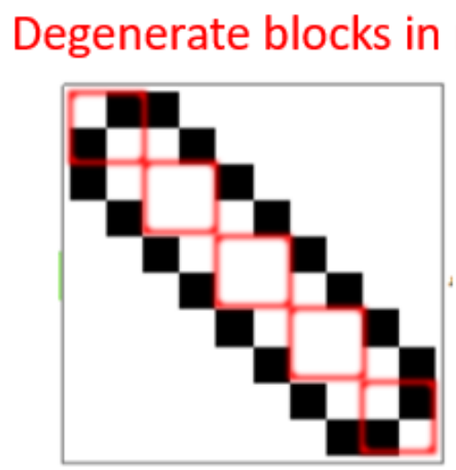

Figure 7: Typical form of a 1st order perturbing Hamiltonian. By considering degenerate PT on the blocks, we always find a K^2 contribution. This goes against the intuition that we can only consider coupling between degenerate states.

We can find the second order contribution from first order terms,

$$E_n^{(2)} = \sum_{m \neq n} \frac{|\langle \phi_n^{(0)}| H |\phi_m^{(0)}\rangle|^2}{E_n^{(0)} - E_m^{(0)}}$$

Thus, we must consider the coupling of all non-degenerate blocks. This is the opposite of the intuition that "only the coupling between degenerate states is relevant". We always get a second order contribution $E \sim K^2$ (there are always states outside of the blocks). For all N, a HOVHS requires tuning a K^2 coefficient. This limits our search for HOVHS, but is not totally devastating.

5 Diagonalizing the Hamiltonian

Here we calculate the dispersions $E_{N,\vec{k}}$ by diagonalizing $H_{N,\vec{k}}$. Calculations stabilize after some matrix order truncation $O(K)$. We

a) Find the dispersion by diagonalizing $H_{N,\vec{k}}$ and expanding it in a power series.

b) Find critical points of the dispersion by setting the coefficients of K and K^2 to 0.

c) Graph the dispersion in some direction $\phi_{\vec{k}}$.

5.1 N=3

a) At $O(K) = 2$, dispersion calculations stabilize,

$$E_{3,\vec{k}} = \begin{cases} k_0 v - W + \frac{k_0 v(9W - 4k_0 v)}{12W} K^2 + ... \\ k_0 v + \frac{W}{2} + F(k_0 v, W, \phi_{\vec{k}})K + G(k_0 v, W, \phi_{\vec{k}})K^2 + ... \\ k_0 v + \frac{W}{2} + H(k_0 v, W, \phi_{\vec{k}})K + J(k_0 v, W, \phi_{\vec{k}})K^2 + ... \end{cases} \tag{60}$$

b) The singlet has a K^2 leading term. We identify the coefficient of K^2 as $\alpha(k_0 v, W) = \frac{k_0 v(9W - 4k_0 v)}{12W}$. By tuning $W \to \frac{4}{9} k_0 v$, we get $\alpha \to 0$, and expect a HOVHS.

The doublet states have dispersions with first and second order terms that do not vanish together, so we do not expect to tune W for a HOVHS for them.

We compare this result to [2]. This requires converting k_0 to real-space distances L, using $k_0 = \frac{Q}{2} \frac{1}{\sin \frac{\pi}{N}}$ and $Q = \frac{4\pi}{\sqrt{3}} \frac{1}{L}$. Making the exchange, we predict a HOVHS at

$$\text{(ours)} \quad W \to 1.86 \frac{v}{L} \tag{61}$$

$$\text{(expected)} \quad W \to 1.36 \frac{v}{L} \tag{62}$$

c) We plot the dispersion for $W = 1.86 \frac{v}{L}$ and various $\phi_{\vec{k}}$. See Figures 8 and 9.

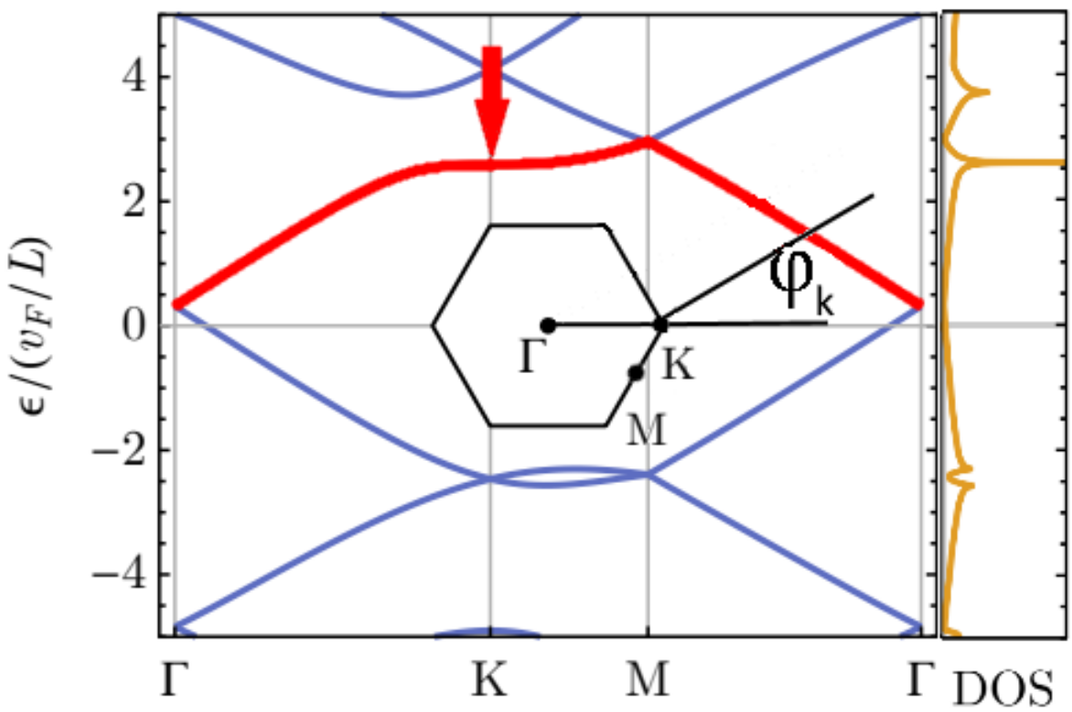

(a)

Figure 8: a) Visual diagram of Brillioun Zone from [2] around the critical potential $W \approx 1.36 \frac{v}{L}$ (we computed this result earlier, and are using Liang's diagrams since they are compact). The dispersion we calculated corresponds to perturbation about the K point in the diagram. The flat band at this point agrees our following calculations.

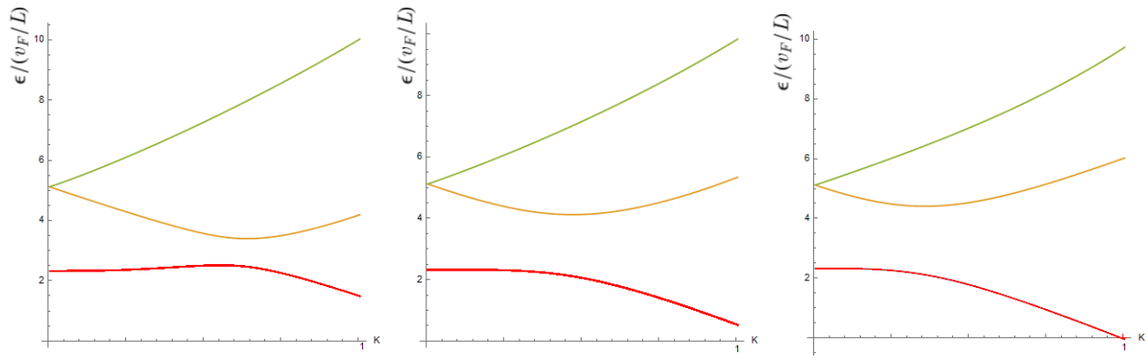

(a) (b) (c)

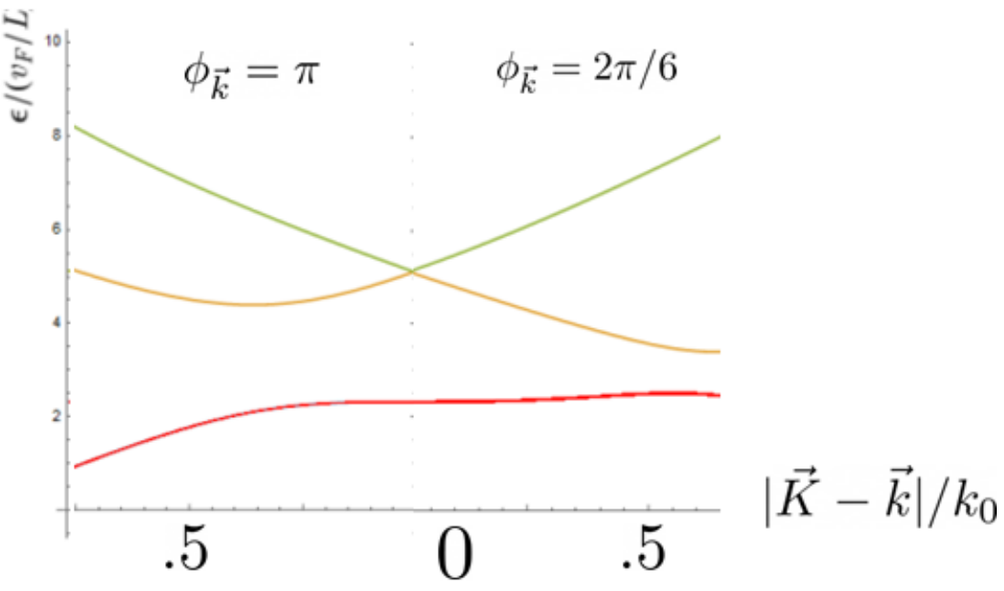

(d)

Figure 9: a) Our computed dispersion $E(K)$ at $\phi_{\vec{k}} = 0$ and critical potential strength $W = \frac{4}{9}k_0 v$. The small expansion parameter $K = k/k_0$ ranges from 0 to 1. The angle $\phi_{\vec{k}} = 0$ is on the line KM. b) $\phi_{\vec{k}} = \pi/6$ c) $\phi_{\vec{k}} = 2\pi/6$, corresponding with the line KΓ. d) The dispersion near the symmetric K point, found by piecing the ΓK result (c) to the KM result (a). This agrees with the expected dispersion.

5.2 N=4

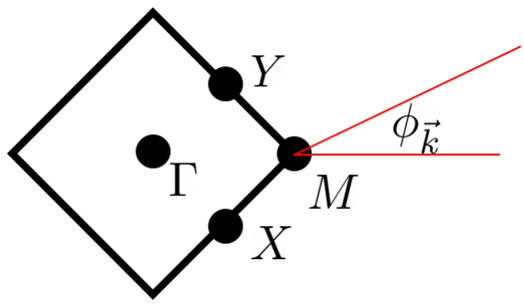

(a)

Figure 10: a) BZ and relevant points for N=4 PT calculations

Let us reference the earlier $N = 4$ computation (Figure 2) for intuition. We expect to find HOVHS on ΓM, and at the mirror symmetric point X (see Figure 10). Thus, we must Taylor expand near but not on the rotationally symmetric point M. This is difficult, and we were only partially able to apply our perturbative results here.

a) We use $O(K) = 4$, so that we can compute high order eigenvalues, even though calculations of $E \sim K^2$ stabilize at $O(K) = 2$. Similar to before, we can see $k_0 = \frac{\sqrt{2}\pi}{L}$. The 4 dispersions about the rotationally symmetric point M take the form,

$$E_{4,\vec{k}} = \begin{cases} k_0 v - W \pm \frac{1}{2}(k_0 v - W)K + \frac{(-k_0^2 v^2 + 2k_0 vW + W^2)}{8W}K^2 + ... \\ k_0 v + W \pm \frac{1}{2}(k_0 v + W)K + \frac{(k_0^2 v^2 + 2k_0 vW - W^2)}{8W}K^2 + ... \end{cases} \tag{63}$$

We have linear and quadratic order terms, and do not expect to tune a single parameter W to realize a HOVHS at M.

To find a HOVHS, we must shift the dispersion so that we are expanding about the HOVHS point $\vec{P}$, with coordinates $\vec{k}'$,

$$\vec{k} \to \vec{P} + \vec{k}' \tag{64}$$

We try to fit P and W so that the coefficients to K and K^2 vanish. This approach is not very successful.

From earlier, we expect a HOVHS near M on ΓM. Here $|\vec{P}| < k_0$ and $\phi_{\vec{k}} = 0$.

We also expect a HOVHS at X. Here $|\vec{P}| = k_0/\sqrt{2}$ and $\phi_{\vec{k}} = \pi/4$.

5.2.1 HOVHS at X

We first unsuccessfully look for the HOVHS at X, which seems easier since we know its exact location P= $.707k_0$, though we still fit for P (this is a large perturbation away from M, and it turns out our PT breaks down). We substitute $K \to P + K'$, and take the coefficients of K' and K'^2. We get two equations

$$f(W, P) = 0 \tag{65}$$
$$g(W, P) = 0 \tag{66}$$

We solve for W_c and P_c that satisfy these relations, and graph the dispersion at $W = W_c$. None of the points are near $P = .707k_0$, and none of the pontentials are near the expected value of $W = 4.8$. Manual tuning does not help. See Figure 11.

It seems the perturbation breaks down before we get to the desired energy level - likely due to requiring $W \ll k_0 v$ in the perturbation, but also we expect $W = 4.71\frac{v}{L} = \frac{4.71}{\sqrt{2}\pi} k_0 v = 1.06 k_0 v$.

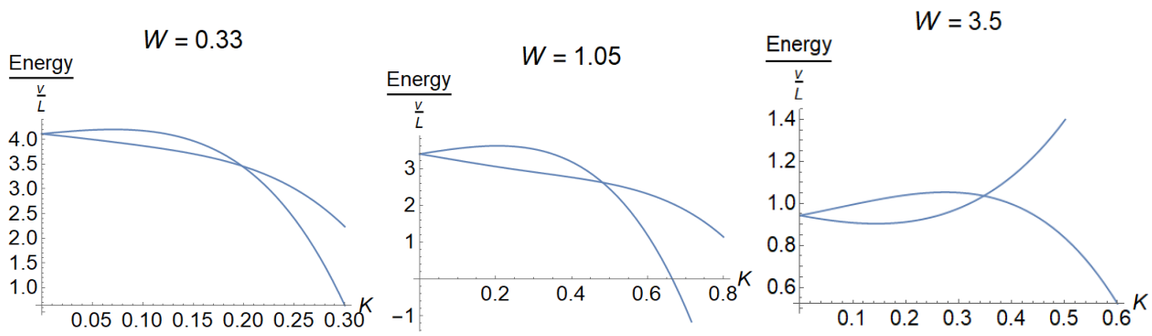

(a) (b) (c)

Figure 11: Here we plot the dispersion at $\phi_{\vec{k}} = \pi/4$ for the W that makes the coefficients K' and K'^2 vanish. We also denote the point P where these vanish. Note that these are 'false positives' and not local minima. a) Plot of lower two bands with $W = .33\frac{v}{L}$, and $P = .1k_0$ b) $W = 1.05\frac{v}{L}$ and $P = .6k_0$. c) Manually tuned potential strength $W = 3.5\frac{v}{L}$ to match energy scale in computation (Figure 2). Note that we expected $W = 4.71\frac{v}{L}$ at $P = k_0/\sqrt{2} = .707k_0$.

5.2.2 HOVHS at M

We somewhat successfully find the HOVHS on ΓM. Again, solving a system of equations for P and W is unsuccessful. We instead tune W manually. See Figure 12. We find,

$$\text{(ours)} \quad W \to 4.07\frac{v}{L} \tag{67}$$

$$\text{(expected)} \quad W \to 4.71\frac{v}{L} \tag{68}$$

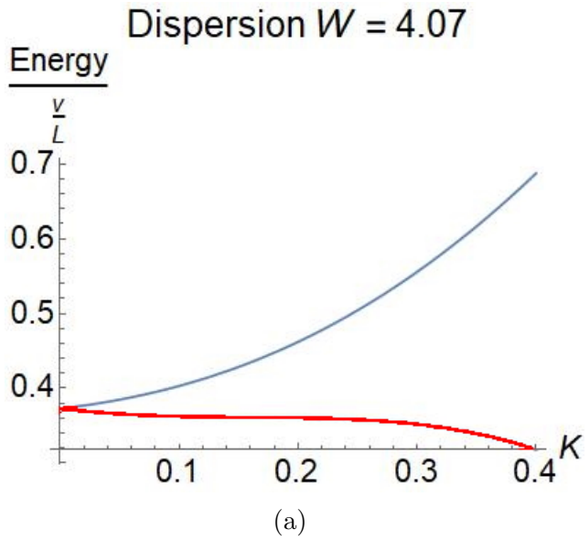

(a)

Figure 12: We manually tuned W to find a flat band on ΓM, as in our computational result (Figure 2). Here $\phi_{\vec{k}} = 0$. The flat band at $W_c = 4.07$ (drawn in red) approximately matches the computed band.

5.3 N=5

a) We use $O(K) = 3$. The singlet dispersion of order K^2 stabilizes at $O(K) = 2$, and K^4 terms stabilize at $O(K) = 3$.

$$E_{5,\vec{k}}(K) = k_0 v - 1.61803W + \frac{k_0 v(0.75W - 0.447214 k_0 v)}{W} K^2 + \left(\frac{0.144721 \mathrm{k0}^4 v^4}{W^3} - \frac{0.46459 \mathrm{k0}^3 v^3}{W^2} + \frac{0.643832 \mathrm{k0}^2 v^2}{W} - 0.165369 \mathrm{k0} v - 0.0406377 W \right) K^4 + F(k_0 v, W, \phi_{\vec{k}}) K^5 + ... \tag{69}$$

This result is consistent with the symmetry argument, (18).

b)

The W that cause K^2 and K^4 terms to vanish are

$$W \to .596 k_0 v \tag{70}$$
$$W \to 1.80 k_0 v \tag{71}$$

This is exciting as we can get a HOVHS with K^4 leading order term, where before we had K^3 leading order term. It seems like the K^2 and K^4 coefficients will vanish for different values of W, and we should not hope for K^5+ leading order term.

c)

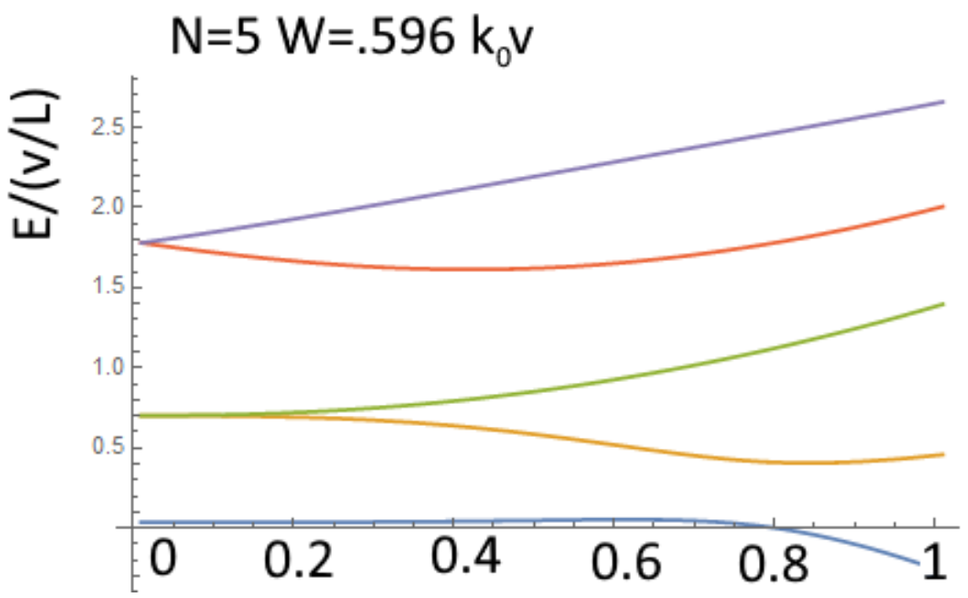

(a)

Figure 13: a) Here we plot the dispersion for $W \to .596 k_0 v$, with $\phi_{\vec{k}} = 0$. We see there is a low-energy K^4 singlet band.

5.4 N > 5

We have not explored $N > 5$ as matrix diagonalization becomes computationally intensive.

From symmetry (18), we expect to always have K^2 and K^4 terms. There is no reason both coefficients should vanish simultaneously. Thus any large value of N will offer the same HOVHS order as $N \geq 4$.

An improvement is to tune more than one parameter. From this analysis, it is theoretically possible with a high N-fold symmetric potential to tune several parameters and realize a very high order VHS.

6 Conclusion

We have seen that in the presence of an N-fold rotationally symmetric potential, we expect to tune the potential strength W to realize HOVHS, where the DOS diverges with power-law exponent $\nu = 3$ (N=3 case) or $\nu = 4$ (N=4 case). When the symmetry N does not produce a crystalline superpotential, we expect even higher order VHS, with $\nu = 4$. Given more tuning parameters, we might expect to find very high order VHS in these systems.

7 Appendix A

7.1 I

Here we show that the dispersion for a N-fold rotationally symmetric potential is $E = \alpha|\vec{k}|^2 + O(|\vec{k}|^3)$

Let us see that first order k terms vanish. Defining $\theta \equiv \frac{2\pi}{N}$,

$$E_N^{(1)}(\vec{k}) = \sum_{n=0}^{N-1} \Omega_x(k_x \cos(n\theta) + k_y \sin(n\theta)) + [''R_{\pi/2}] \tag{72}$$

$$= \Omega_x k_x \sum_{n=0}^{N-1} \cos(n\theta) + \Omega_x k_y \sum_{n=0}^{N-1} \sin(n\theta) + [''R_{\pi/2}] \tag{73}$$

$$= 0 \tag{74}$$

Second order terms go isotropically as $k^2 = k_x^2 + k_y^2$,

$$E_N^{(2)}(\vec{k}) = \sum_{n=0}^{N-1} \alpha_{xx}(k_x \cos(n\theta) + k_y \sin(n\theta))^2 + [''R_{\pi/2}] \tag{75}$$

$$+ \sum_{n=0}^{N-1} \alpha_{xy}(k_x \cos(n\theta) + k_y \sin(n\theta))(k_y \cos(n\theta) - k_x \sin(n\theta)) \tag{76}$$

$$... = \alpha k^2 \tag{77}$$

Let us confirm this final step. We'll find that (75) goes as k^2, while (76) vanishes.

(75) is equal to $\alpha_{xx} \sum_n k_x^2 \cos^2(n\theta) + k_y^2 \sin^2(n\theta) + 2k_x k_y \cos(n\theta)\sin(n\theta) + [''R_{\pi/2}]$. Odd terms like $\sum_n \cos(n\theta)\sin(n\theta) \sim \sum_n \sin(2n\theta)$ sum to 0, while the even terms $\sum_n \sin^2(n\theta) = \sum_n \cos^2(n\theta) = n/2$ sum to a constant. Enforcing these sums and then evaluating the $[''R_{\pi/2}]$ term, (75) is $\sim [\alpha_{xx} + \alpha_{yy}] \sum_n \left(k_x^2 + k_y^2\right) \sim k^2$. We see that (76) is equal to $\alpha_{xy} \sum_n \left[k_x k_y(\cos^2(n\theta) - \sin^2(n\theta)) + (k_x^2 - k_y^2)(\cos(n\theta)\sin(n\theta))\right]$ which vanishes using the sums found before.

We are done, and do not need to account for mirror symmetry as it is automatically obeyed.

7.2 II

Here we confirm that rotational and mirror symmetric systems create HOVHS more easily. Namely, we expect to tune one or two parameters to create HOVHS. We use the formal definition of HOVHS (11).

7.2.1 rotation symmetry

For an expansion about the 3-fold symmetric point K (Figure 1), we have

$$E(K_x + k_x, K_y + k_y) - E(k_x, k_y) = a(k_x^2 + k_y^2) + b(k_x^3 - 3k_x k_y^2) + gk^4 + ... \tag{78}$$

$$\frac{\partial E}{\partial k_x} = 0 = 2akx + b(3kx^2 - 3ky^2) + 4gkx(kx^2 + ky^2) + ... \tag{79}$$

$$\frac{\partial E}{\partial k_y} = 0 = 2aky - 6bkxky + 4gky(kx^2 + ky^2) + ... \tag{80}$$

$$\det(D) = 0 = 4a^2 + (-36b^2 + 32ag)kx^2 - 48bgkx^3 + 48g^2kx^4 + ... \tag{81}$$

One solution is $a = k_x = k_y = 0$. Clearly there a HOVHS at K requires tuning one coefficient a, thus likely one parameter W.

This result holds for any N, not just $N = 3$, since we know that any rotationally symmetric potential has leading order k^2.

7.2.2 mirror symmetry

For an expansion about P mirror-symmetric line with k_x parallel and k_y perpendicular to the line, we have

$$E(P_x + k_x, P_y + k_y) - E(k_x, k_y) = ak_x + bk_x^2 + ck_y^2 + dk_x^3 + ek_xk_y^2 + fk_x^4 + gk_x^2k_y^2 + hk_y^4 + ... \tag{82}$$

$$\frac{\partial E}{\partial k_x}|_{k_y=0} = 0 = a + 2bk_x + 3dk_x^2 + 4fk_x^3 + ... \tag{83}$$

$$\frac{\partial E}{\partial k_y}|_{k_y=0} = 0 = 0 \text{ (always holds)} \tag{84}$$

$$\begin{aligned}\det(D)|_{k_y=0} = 0 = 4bc + (12cd + 4be)k_x + (12de + 24cf + 4bg)k_x^2 \\ + (24ef + 12dg)k_x^3 + 24fgk_x^4 + ...\end{aligned} \tag{85}$$

We assume $k_y = 0$ because we want a VHS on the mirror-symmetric line. Clearly tuning 2 coefficients $a = b = 0$ or $a = c = 0$ and $k = k_x = 0$ satisfies it. Or we can choose some k_x to satisfy one eqn, and some coefficient to satisfy the other, to tune a single coefficient (the conditions for a solution for roots of k_x is complicated and may not be real). So it is not clear if tuning just 1 coefficient (or harder yet, 1 parameter) will satisfy the 3 HOVHS conditions.

8 Appendix B

We cover perturbations in k-space here, deriving H^W (more difficult), then H^v (easier).

8.1 H^W term

8.1.1 n basis series expansion

Here we substitute (43-45) into (39) to find $H^W_{N,\vec{k}}$ as a power series in small $K = k/k_0$.

For convenience we copy (39),

$$H^W_N = W \sum_n e^{-i\frac{(\phi_{n+1}-\phi_n)}{2}} \cos\frac{(\phi_{n+1} - \phi_n)}{2} |n+1\rangle \langle n| + H.c.$$

Expressing (43) as a power series,

$$\phi_n \to \phi'_n = \arctan(\frac{\sin(\phi_n) + Ksin(\phi_{\vec{k}})}{\cos(\phi_n) + K\cos(\phi_{\vec{k}})}) \tag{86}$$

$$\approx \phi_n + \sum_{j=1}^{\infty} \frac{(-1)^{j+1}}{j} K^j \sin[j(\phi_{\vec{k}} - \phi_n)] \tag{87}$$

The difference of perturbed angles can be written as

$$\frac{\phi'_{n+1}-\phi'_n}{2} = \frac{\pi}{N} + \frac{1}{2}\sum_{j=1}^{\infty}\frac{(-1)^{j+1}}{j}K^j\left[\sin[j(\phi_{\vec{k}}-\phi_n-\frac{2\pi}{N})]-\sin[j(\phi_{\vec{k}}-\phi_n)]\right] \tag{88}$$

$$= \frac{\pi}{N} + \frac{1}{2}\sum_{j=1}^{\infty}\frac{(-1)^{j+1}}{j}K^j\left[-2\sin(\frac{j\pi}{N})\cos[j(\phi_{\vec{k}}-\phi_n-\frac{\pi}{N})]\right] \tag{89}$$

$$= \frac{\pi}{N} - \Lambda_{n,\vec{k}}(K) \tag{90}$$

Where we have defined (we will use $\vec{k}$ subscripts implicitly, but we include them here for clarity)

$$\Lambda_{n,\vec{k}}(K) \equiv \sum_{j=1}^{\infty}\lambda_j c_{n,\vec{k}}(j)K^j \tag{91}$$

$$\lambda_j \equiv \frac{(-1)^{j+1}}{j}\sin(\frac{j\pi}{N}) \tag{92}$$

$$c_{n,\vec{k}}(j) \equiv \cos[j(\phi_{\vec{k}}-\phi_n-\frac{\pi}{N})] \tag{93}$$

Now we can use the infinite sum $\Lambda_n(K) \ll 1$ as an expansion parameter,

$$H_N^W = W\sum_{n=0}^{N-1}\left[e^{i(\frac{\pi}{N}-\Lambda_n)}\cos(\frac{\pi}{N}-\Lambda_n)\right]|n+1'\rangle\langle n'| + H.c. \tag{94}$$

$$\approx W\sum_{n=0}^{N-1}\left[e^{-i\frac{\pi}{N}}\cos(\frac{\pi}{N}) + \frac{e^{-\frac{2\pi i}{N}}}{2}\sum_{l=1}^{\infty}D_l(\Lambda_n)^l\right]|n+1'\rangle\langle n'| + H.c. \tag{95}$$

where

$$D_l \equiv \frac{(2i)^l}{l!} \tag{96}$$

We can stop here, but for proofs it is useful to simplify the double sum $\sum_l D_l(\Lambda_n)^l$ (there are two infinite sums - the sum over l and an internal sum in Λ_n). We can write all terms in the double sum as some power of K times some coefficient χ_n. Thus we would like to replace the double sum with a single sum $\sum_{x=1}^{\infty}\chi_n(x)K^x$.

$$\sum_{x=1}^{\infty}\chi_n(x)\cdot K^x \equiv \sum_{l=1}^{\infty}D_l\cdot(\Lambda_n)^l \tag{97}$$

We must find the coefficients $\chi_n(x)$ that satisfy this.

It is useful to define

$$b_n(j) \equiv \lambda_j c_n(j) \tag{98}$$

so that

$$\Lambda_n = \sum_{j=1}^{\infty}b_n(j)\cdot K^j \tag{99}$$

We now solve for $\chi_n(x)$ (suppressing the subscript n),

$$\sum_{x=1}^{\infty}\chi(x)K^x = \sum_{l=1}^{\infty}D_l(\Lambda)^l = \sum_{l=1}^{\infty}D_l\Big(\sum_{j=1}^{\infty}b(j)K^j\Big)^l \tag{100}$$

$$= \sum_{l=1}^{\infty}D_l\Big(b(1)K + b(2)K^2 + b(3)K^3 + ...\Big)^l \tag{101}$$

Let us solve (101). The contribution of the expansion power l to to the term of order K^x is

$$A_0 \cdot D_l \cdot \Big[(b(1)K)^{pow_1} \cdot (b(2)K^2)^{pow_2} \cdot (b(3)K^3)^{pow_3} ...\Big] \tag{102}$$

where we have the constraints,

$$pow_1 + 2pow_2 + 3pow_3 + ... = x \tag{103}$$
$$pow_1 + pow_2 + pow_3 + ... = l \tag{104}$$

There is a connection here to partitions from number theory - all the ways of breaking a positive integer into other positive integers. The terminology is best shown by example. The "partitions" of the number 4 are: 1+1+1+1, 1+1+2, 1+3, 2+2, and 4. Each term in a partition is a "part". For instance, 1+1+2 has three parts, where the parts of length 1 (the 1+1) have a degeneracy of 2, and the part of length 2 has a degeneracy of 1.

In general, a single partition of x, p_x, is described by a set of length-degeneracy pairs (i,d_i) such that $\sum_i i \cdot d_i = x$. Of course, the lengths are integers $i > 0$, and degeneracies are integers $d_i \geq 0$ ($d_i = 0$ means no parts of length i are present). The following is a natural definition (no two pairs will share the same length i),

$$p_x = \{(i, d_i)\}_{\sum_i i \cdot d_i = x}^{i>0} \tag{105}$$

Now we can apply this terminology. Using (103), pow_i are the degeneracies of the part lengths i in the partition of x. Thus, $pow_i = d_i$, and also b terms are of the form $b(i)^{d_i}$. Using (104), we also see this partition contains l total parts. We sum over all l, so every possible partition of x is considered.

We can also find the multinomial degeneracy factor in the language of partitions. For example, $(a+b+c)^l = \sum_{n_1+n_2+n_3=l} \frac{l!}{n_1!n_2!n_3!} a^{n_1} b^{n_2} c^{n_3}$. In our case, a partition on x of l total parts, with $u \leq l$ of them unique, gives a degeneracy factor $A_0 = \frac{l!}{\prod_{u_i} degeneracy(u_i)!}$.

Using all of this,

$$\chi(x) = \sum_{\substack{\text{partition}_i \in \\ \text{all partitions of } x}} \left[D_{(\substack{\#\text{ parts} \\ \text{in partition}_i})} \frac{(\#\text{ parts in partition}_i)!}{\prod_{\substack{\text{part length}_j \\ \in \text{partition}_i}} (\#\text{ parts with length}_j)!} \right] \cdot \left(\prod_{\substack{\text{part length j} \in \\ \text{partition}_i}} b(\text{length j})^{\#\text{ parts with length}_j} \right) \tag{106}$$

More concisely and unsurpressing subscripts,

$$\chi_{n,\vec{k}}(x) = \sum_{\substack{\text{all } p_x = \{(i,d_i)\} \\ \text{s.t. } \sum_i i \cdot d_i = x}} \left[D_{L_0} \frac{L_0!}{\prod_{(i,d_i)\in p_x} d_i!} \right] \left(\prod_{(i,d_i)\in p_x} (b_{n,\vec{k}}(i))^{d_i} \right) \tag{107}$$

where

$$L_0 \equiv \sum_{i>0} d_i \tag{108}$$

is the total number of parts in p_x.

We can now write the Hamiltonian as,

$$H^W_{N,\vec{k}} = W \sum_{n=0}^{N-1} \left(e^{-\frac{\pi i}{N}} \cos(\frac{\pi}{N}) + \frac{e^{-\frac{2\pi i}{N}}}{2} \sum_{x=1}^{\infty} \chi_{n,\vec{k}}(x) \cdot K^x \right) |n+1'\rangle \langle n'| + H.c. \tag{109}$$

8.1.2 n to j basis expansion

Here we insert (45) into (109). This is just a change of basis, and (45) takes a familiar form,

$$|n'\rangle = \frac{1}{\sqrt{N}} \sum_{j=0}^{N-1} e^{-\frac{2\pi i n}{N} j} |j'\rangle \tag{110}$$

From now on we suppress the prime and write $|j'\rangle$ as $|j\rangle$. Primes will indicate dummy sum indexes, and all states are the "new" states.

We already know the answer to the K^0th order $H^W_{N,\vec{k}}$ (41). Let's only focus on the higher order terms.

We now have a form for the Hamiltonian,

$$H^{W\ (x>0)}_{N,\vec{k}} = W \sum_{n=0}^{N-1} \left(\frac{e^{-\frac{2\pi i}{N}}}{2} \sum_{x=1}^{\infty} \chi_{n,\vec{k}}(x) \cdot K^x \right) \left(\frac{1}{\sqrt{N}} \sum_{j'=0}^{N-1} e^{-\frac{2\pi i (n+1)}{N} j'} |j'\rangle \right) \left(\frac{1}{\sqrt{N}} \sum_{j=0}^{N-1} e^{\frac{2\pi i n}{N} j} \langle j| \right) + H.c. \tag{111}$$

$$= W \frac{e^{-\frac{2\pi i}{N}}}{2} \sum_{x=1}^{\infty} K^x \sum_{j,j'=0}^{N-1} e^{-\frac{2\pi i}{N} j'} |j'\rangle \langle j| \left[\frac{1}{N} \sum_{n=0}^{N-1} e^{-\frac{2\pi i n}{N}(j'-j)} \chi_{n,\vec{k}}(x) \right] + H.c. \tag{112}$$

Analytically we could stop here. To compute the Hamiltonian explicitly, we must do more work.

8.1.3 decomposition

To simplify further, we must evaluate the term in brackets using an orthogonality relation, on the variable n.

However, the n-dependent part of $\chi_n(x)$ contains complicated products of cosine terms $\chi \sim \cos(a)^p \cos(b)^q ....$

We resolve this by decomposing these products into sums of single cosine terms to some power $\chi \sim \sum \cos(a_i)^{p_i}$ by repeatedly using

$$\cos(a)\cos(b) = \frac{1}{2}[\cos(a+b) + \cos(a-b)] \tag{113}$$

For example, let's decompose $\chi_n(3)$. The partitions of 3 are $1+1+1$, 3, and $1+2$. From the definition of partitions (105), $p_3 = \{(1,3)\}$ or $\{(3,1)\}$ or $\{(1,1),(2,1)\}$.

From the definition of χ (107), the n-dependent parts (suppressing the subscripts and ignoring constants) are $\chi(3) \sim c(1)^3 + c(3) + c(1)c(2)$

We can simplify the product using cosine rule, $c(1)c(2) \sim c(1) + c(3)$

Thus $\chi(3) \sim c(1)^3 + c(3) + c(1)$

We can do this for any $\chi(x)$. The decomposition will take the form,

$$\chi_n(x) = \sum_{\theta(x)} \gamma_\theta \cdot c_n(M_\theta)^{L_\theta} \tag{114}$$

where M, L are integers.

It is easy to compute γ_θ in mathematica using recursion.

8.1.4 orthogonality

We want to evaluate the bracket term in (112), assuming the decomposition (114).

To do this, we need the relation

$$\frac{1}{N}\sum_n \cos^L\left(M(\phi_{\vec{k}}-\phi_n-\frac{\pi}{N})\right)e^{-\frac{2\pi i n}{N}(j'-j)} \tag{115}$$

Expanding the cosine in terms of exponentials and using binomial expansion over dummy variable q, we get

$$=(\frac{1}{2})^L\sum_{q=0}^{L}\binom{L}{q}e^{-i(\phi_{\vec{k}}-\frac{\pi}{N})M(L-2q)}\left[\frac{1}{N}\sum_n e^{\frac{2\pi i}{N}nM(L-2q)}e^{-\frac{2\pi i}{N}n(j'-j)}\right] \tag{116}$$

Where the term in brackets is $\delta_{[M(L-2q)=j'-j]}$.

We need to find a hermitian conjugate somewhere. We see that $L-2q$ goes from $-L, -L+2, -L+4, ..., L-4, L-2, L$. Let us define $z=L-2q$ and consider only positive z. This should do the trick.

$$=(\frac{1}{2})^L\left(\sum_{q=0}^{\text{floor}(L/2)}+\sum_{\text{floor}(L/2)+1}^{L}\right) \tag{117}$$

$$=(\frac{1}{2})^L\sum_{z=L,L-2,...}^{z\geq 0}\binom{L}{(L-z)/2}[1-\frac{1}{2}\delta_{z=0}]\left[e^{-i(\phi_{\vec{k}}-\frac{\pi}{N})Mz}\delta_{Mz=j'-j}+e^{i(\phi_{\vec{k}}-\frac{\pi}{N})Mz}\delta_{-Mz=j'-j}\right] \tag{118}$$

We account for double counting at 0 with the $[1-\frac{1}{2}\delta_{z=0}]$ term.

Thus (115) = (118). More concisely,

$$\begin{aligned}&\frac{1}{N}\sum_{n=0}^{N-1}e^{-\frac{2\pi i n}{N}(j'-j)}\left[c_{n,\vec{k}}(M)\right]^L\\&\quad=\sum_{z=L,L-2,...}^{z\geq 0}\xi_2(L,z)\cdot e^{-i(\phi_{\vec{k}}-\frac{\pi}{N})Mz}\cdot\delta_{(Mz=j'-j)}+[''z\to -z]\end{aligned} \tag{119}$$

where

$$\xi_2(L,z)\equiv(\frac{1}{2})^L\binom{L}{(L-z)/2}[1-\frac{1}{2}\delta_{z=0}] \tag{120}$$

8.1.5 j basis with decomposition

Let us simplify the Hamiltonian (112). We first insert our decomposition (114),

$$H^{W\ (x>0)}_{N,\vec{k}}=W\frac{e^{-\frac{2\pi i}{N}}}{2}\sum_{x=1}^{\infty}K^x\sum_{\theta(x)}\gamma_\theta\sum_{j,j'=0}^{N-1}e^{-\frac{2\pi i}{N}j'}\left|j'\right\rangle\left\langle j\right|\left[\frac{1}{N}\sum_{n=0}^{N-1}e^{-\frac{2\pi i n}{N}(j'-j)}[c_{n,\vec{k}}(M_\theta)]^{L_\theta}\right]+H.c. \tag{121}$$

Next we use orthogonality (119),

$$= W\frac{e^{-\frac{2\pi i}{N}}}{2}\sum_{x=1}^{\infty}K^x\sum_{\theta(x)}\gamma_\theta\sum_{j,j'=0}^{N-1}e^{-\frac{2\pi i}{N}j'}\left|j'\right\rangle\left\langle j\right| \cdot\left[\sum_{z=L_\theta,L_\theta-2,\ldots}^{z\geq 0}\xi_2(L_\theta,z)\cdot e^{-i(\phi_{\vec{k}}-\frac{\pi}{N})M_\theta z}\cdot\delta_{(M_\theta z=j'-j)}+\left[''z\rightarrow -z\right]\right]+H.c. \tag{122}$$

Rearranging terms,

$$= W\frac{e^{-\frac{2\pi i}{N}}}{2}\sum_{x=1}^{\infty}K^x\sum_{\theta(x)}\gamma_\theta \cdot\left(\left[\sum_{z=L_\theta,L_\theta-2,\ldots}^{z\geq 0}\xi_2(L_\theta,z)\cdot e^{-i(\phi_{\vec{k}}-\frac{\pi}{N})M_\theta z}\cdot\sum_{j,j'=0}^{N-1}\delta_{(M_\theta z=j'-j)}e^{-\frac{2\pi i}{N}j'}\left|j'\right\rangle\left\langle j\right|\right]+\left[''z\rightarrow -z\right]\right)+H.c. \tag{123}$$

Enforcing the delta function on $j'=j+Mz$,

$$H^{W\ (x>0)}_{N,\vec{k}} = W\frac{e^{-\frac{2\pi i}{N}}}{2}\sum_{x=1}^{\infty}K^x\sum_{\theta(x)}\gamma_\theta \cdot\left(\left[\sum_{z=L_\theta,L_\theta-2,\ldots}^{z\geq 0}\xi_2(L_\theta,z)\cdot e^{-i(\phi_{\vec{k}}-\frac{\pi}{N})M_\theta z}\cdot\sum_{j=0}^{N-1}e^{-\frac{2\pi i}{N}(j+M_\theta z)}\left|j+M_\theta z\right\rangle\left\langle j\right|\right]+\left[''z\rightarrow -z\right]\right)+H.c. \tag{124}$$

Simplifying phase, we have

$$H^{W\ (x>0)}_{N,\vec{k}} = W\frac{e^{-\frac{2\pi i}{N}}}{2}\sum_{x=1}^{\infty}K^x\sum_{\theta(x)}\gamma_\theta \cdot\left(\left[\sum_{z=L_\theta,L_\theta-2,\ldots}^{z\geq 0}\xi_2(L_\theta,z)\cdot e^{-i(\phi_{\vec{k}}+\frac{\pi}{N})M_\theta z}\cdot\sum_{j=0}^{N-1}e^{-\frac{2\pi i}{N}j}\left|j+M_\theta z\right\rangle\left\langle j\right|\right]+\left[''z\rightarrow -z\right]\right)+H.c. \tag{125}$$

8.2 H^v term

8.2.1 n basis series expansion

Here we substitute (43-45) into (35) to find $H^v_{N,\vec{k}}$ as a power series in small $K=k/k_0$.

We have

$$H^v_{N,\vec{k}} = v\sum_{n=0}^{N-1}\sqrt{|\vec{k}_n+\vec{k}|^2}\left|n'\right\rangle\left\langle n'\right| \tag{126}$$

We see that $|\vec{k}_n+\vec{k}|^2 = (k_0\cos\theta_n+k\cos\phi_{\vec{k}})^2+(k_0\sin\theta_n+k\sin\phi_{\vec{k}})^2 = (k_0)^2+k^2+2k_0k(\cos\theta_n\cos\phi_{\vec{k}}+\sin\theta_n\sin\phi_{\vec{k}}) = (k_0)^2+k^2+2k_0k(\cos(\phi_{\vec{k}}-\phi_n))$. Thus,

$$H^v_{N,\vec{k}} = vk_0 \sum_{n=0}^{N-1} \sqrt{1 + 2K\cos(\phi_{\vec{k}} - \phi_n) + K^2}\, |n'\rangle \langle n'| \tag{127}$$

$$= vk_0 \sum_{n=0}^{N-1} \Big(\sum_{m=0}^{\infty} C_m (2K\cos(\phi_{\vec{k}} - \phi_n) + K^2)^m \Big) |n'\rangle \langle n'| \tag{128}$$

$$= vk_0 \sum_{n=0}^{N-1} \sum_{m=0}^{\infty} C_m \Big(\sum_{l=0}^{m} \binom{m}{l} \cdot [2K\cos(\phi_{\vec{k}} - \phi_n)]^l \cdot K^{2(m-l)} \Big) |n'\rangle \langle n'| \tag{129}$$

$$= vk_0 \sum_{n=0}^{N-1} \sum_{m=0}^{\infty} \sum_{l=0}^{m} C_{m,l} \cdot [2K\cos(\phi_{\vec{k}} - \phi_n)]^l \cdot K^{2(m-l)} |n'\rangle \langle n'| \tag{130}$$

$$= vk_0 \sum_{m=0}^{\infty} \sum_{l=0}^{m} C_{m,l} \cdot 2^l K^{2m-l} \sum_{n=0}^{N-1} \cos^l(\phi_{\vec{k}} - \phi_n) |n'\rangle \langle n'| \tag{131}$$

Where we have defined

$$C_{m,l} \equiv \binom{m}{l} \cdot C_m \tag{132}$$

$$C_m \equiv \frac{1}{m!} \cdot (\frac{1}{2})!_m \tag{133}$$

$$(\frac{1}{2})!_m \equiv \frac{1}{2}(\frac{1}{2} - 1)(\frac{1}{2} - 2)...(\frac{1}{2} - (m-1)) \tag{134}$$

8.2.2 n to j basis expansion

Substituting the plane wave basis (45),

$$H^v_{N,\vec{k}} = vk_0 \sum_{j,j'=0}^{N-1} |j'\rangle \langle j| \sum_{m=0}^{\infty} \sum_{l=0}^{m} C_{m,l} \cdot 2^l K^{2m-l} \left[\frac{1}{N} \sum_{n=0}^{N-1} e^{-\frac{2\pi i n}{N}(j'-j)} \cos^l(\phi_{\vec{k}} - \phi_n) \right] \tag{135}$$

Using orthogonality (119),

$$H^v_{N,\vec{k}} = vk_0 \sum_{j,j'=0}^{N-1} |j'\rangle \langle j| \sum_{m=0}^{\infty} \sum_{l=0}^{m} C_{m,l} \cdot 2^l K^{2m-l} \left[\sum_{z=l,l-2,...}^{z\geq 0} \xi_2(l,z) \cdot e^{-\imath\phi_{\vec{k}} z} \cdot \delta_{(z=j'-j)} + [''z \to -z] \right] \tag{136}$$

$$= vk_0 \sum_{m=0}^{\infty} \sum_{l=0}^{m} C_{m,l} \cdot 2^l K^{2m-l} \sum_{z=l,l-2,...}^{z\geq 0} \xi_2(l,z) \cdot e^{-\imath\phi_{\vec{k}} z} \sum_{j=0}^{N-1} |j+z\rangle \langle j| + [''z \to -z] \tag{137}$$

$$= vk_0 \sum_{m=0}^{\infty} \sum_{l=0}^{m} K^{2m-l} \sum_{z=l,l-2,...}^{z\geq 0} \Big[C_{m,l} \cdot \binom{l}{(l-z)/2} [1 - \frac{1}{2}\delta_{z=0}] \Big] \cdot e^{-\imath\phi_{\vec{k}} z} \sum_{j=0}^{N-1} |j+z\rangle \langle j| + H.c. \tag{138}$$

$$= vk_0 \sum_{m=0}^{\infty} \sum_{l=0}^{m} K^{2m-l} \sum_{z=l,l-2,...}^{z\geq 0} \xi_1(m,l,z) \cdot e^{-\imath\phi_{\vec{k}} z} \sum_{j=0}^{N-1} |j+z\rangle \langle j| + H.c. \tag{139}$$

$$\tag{140}$$

Defining

$$\xi_1(m,l,z) \equiv C_{m,l} \cdot \binom{l}{(l-z)/2} [1 - \frac{1}{2}\delta_{z=0}] \tag{141}$$

Lastly, we can substitute $x = 2m - l$ for more convenient powers of K,

$$H^{v}_{N,\vec{k}} = vk_0 \sum_{m=0}^{\infty} \sum_{x=m}^{2m} K^x \sum_{\substack{z=2m-x,\\ 2m-x-2,\\ 2m-x-4,\\ \dots}}^{z\geq 0} \xi_1(m, 2m-x, z) \cdot e^{-\imath\phi_{\vec{k}} z} \sum_{j=0}^{N-1} |j+z\rangle \langle j| + H.c. \tag{142}$$

References

[1] J. Cano, S. Fang, J. H. Pixley, and J. H. Wilson, "Moiré superlattice on the surface of a topological insulator", Physical Review B **103**, 10.1103/physrevb.103.155157 (2021).

[2] T. Wang, N. F. Yuan, and L. Fu, "Moiré surface states and enhanced superconductivity in topological insulators", Physical Review X **11**, 10.1103/physrevx.11.021024 (2021).

[3] X.-L. Qi and S.-C. Zhang, "Topological insulators and superconductors", Reviews of Modern Physics **83**, 1057–1110 (2011).

[4] M. Z. Hasan and C. L. Kane, "Icolloquium/i: topological insulators", Reviews of Modern Physics **82**, 3045–3067 (2010).

[5] R. Bistritzer and A. H. MacDonald, "Moiré bands in twisted double-layer graphene", Proceedings of the National Academy of Sciences **108**, 12233–12237 (2011).

[6] Y. Cao, V. Fatemi, S. Fang, K. Watanabe, T. Taniguchi, E. Kaxiras, and P. Jarillo-Herrero, "Unconventional superconductivity in magic-angle graphene superlattices", Nature **556**, 43–50 (2018).

[7] A. Dunbrack and J. Cano, "Magic angle conditions for twisted three-dimensional topological insulators", Physical Review B **106**, 10.1103/physrevb.106.075142 (2022).

[8] A. Chandrasekaran, A. Shtyk, J. J. Betouras, and C. Chamon, "Catastrophe theory classification of fermi surface topological transitions in two dimensions", Physical Review Research **2**, 10.1103/physrevresearch.2.013355 (2020).

[9] N. F. Q. Yuan and L. Fu, "Classification of critical points in energy bands based on topology, scaling, and symmetry", Phys. Rev. B **101**, 125120 (2020).

[10] C. Forsythe, X. Zhou, K. Watanabe, T. Taniguchi, A. Pasupathy, P. Moon, M. Koshino, P. Kim, and C. R. Dean, "Band structure engineering of 2d materials using patterned dielectric superlattices", Nature Nanotechnology **13**, 566–571 (2018).

[11] M. V. Jari ć, "Diffraction from quasicrystals: geometric structure factor", Phys. Rev. B **34**, 4685–4698 (1986).